Supporting Information

Highly Durable Solid Oxide Fuel Cells: Suppressing Chemical Degradation via Rational Design of Diffusion-blocking Layer

Seunghwan Lee[a,b], Sanghyeok Lee[a,c], Hyo-Jin Kim[a,d], Sung Min Choi[a], Hyegsoon An[a,e], Mi Young Park[a,d], Jisu Shin[a,f], Jung Hoon Park[a,g], Junsung Ahn[a,h], Donghwan Kim[a,c], Ho-Il Ji[a], Hyoungchul Kim[a], Ji-Won Son[a], Jong-Ho Lee[a], Byung-Kook Kim[a], Hae-Weon Lee[a], Jongsup Hong[i], Dongwook Shin[b] and Kyung Joong Yoon[a,*]

[a]High-Temperature Energy Materials Research Center,
Korea Institute of Science and Technology, Seoul, Korea

[b]Division of Materials Science and Engineering, Hanyang University, Seoul, Korea

[c]Department of Mechanical Engineering, Korea University, Seoul, Korea

[d]Department of Materials Science and Engineering, Korea University, Seoul, Korea

[e]Department of Fuel Cells and Hydrogen Technology, Hanyang University, Seoul, Korea

[f]Department of energy engineering, Hanyang University, Seoul, Korea

[g]Graduate School of EEWS, Korea Advanced Institute of Science and Technology,
Daejeon, Korea

[h]Department of Materials Science and Engineering, Seoul National University, Seoul, Korea

[i]School of Mechanical Engineering, Yonsei University, Seoul, Korea

*Corresponding Author at:

Korea Institute of Science and Technology

High-Temperature Energy Materials Research Center

Hwarangno 14-gil 5, Seongbuk-gu, Seoul 136-791, Korea

Tel: +82-2-958-5515

Fax: +82-2-958-5529

E-mail: kjyoon@kist.re.kr

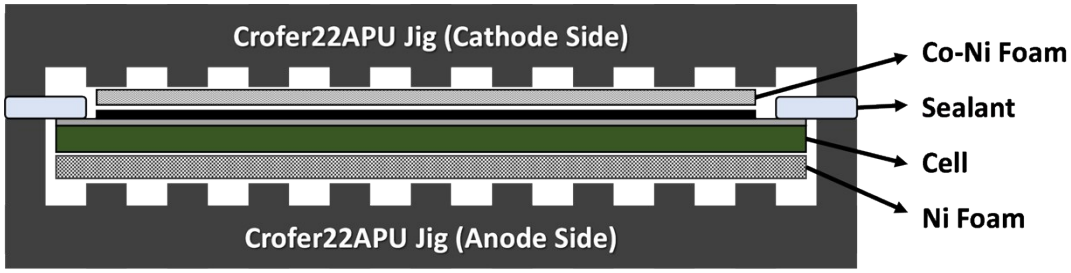

Figure S1. Schematic of test setup composed of the anode-supported planar cell, Crofer 22 APU testing fixtures, glass–ceramic sealant, Co–Ni foam cathode current collector, and Ni foam anode current collector.

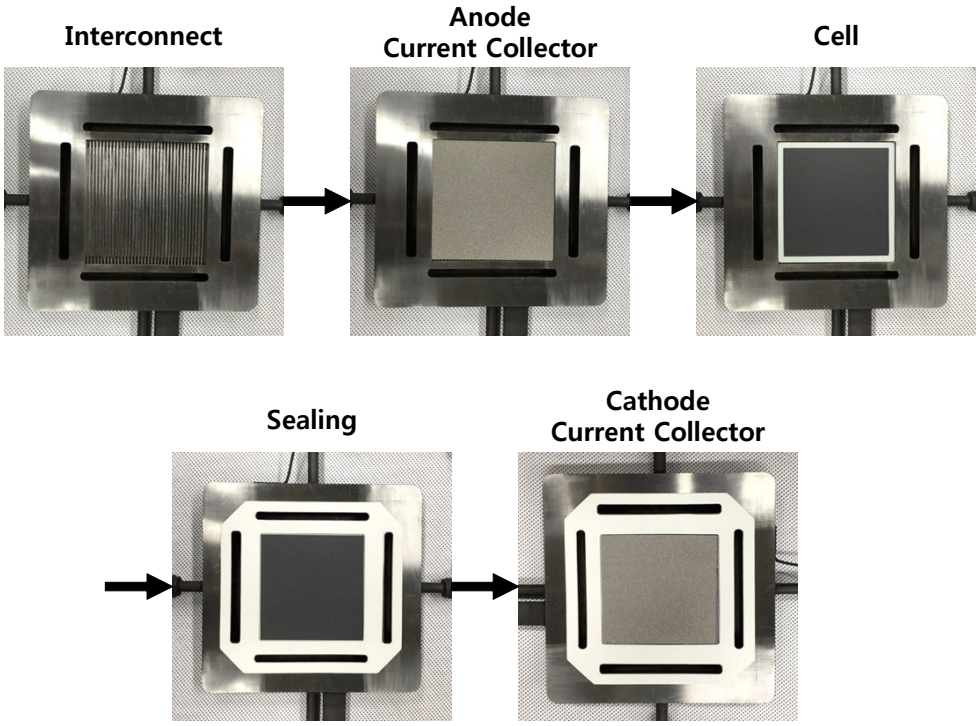

Figure S2. Stack assembly procedures using 10 cm × 10 cm cell, Crofer 22 APU interconnect, glass–ceramic sealant, Co–Ni foam cathode current collector and Ni foam anode current collector.

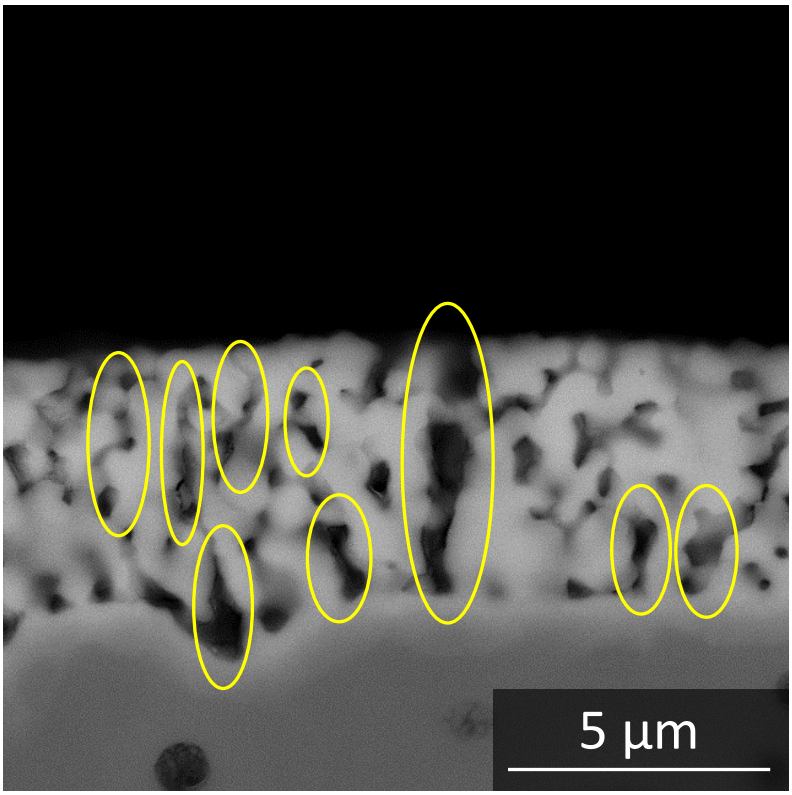

Figure S3. SEM image of the GDC interlayer fabricated using nanoparticles on a pre-sintered YSZ electrolyte substrate. A significant number of vertically aligned pores were formed owing to the nonuniform particle packing and restriction in the lateral shrinkage during constrained sintering.

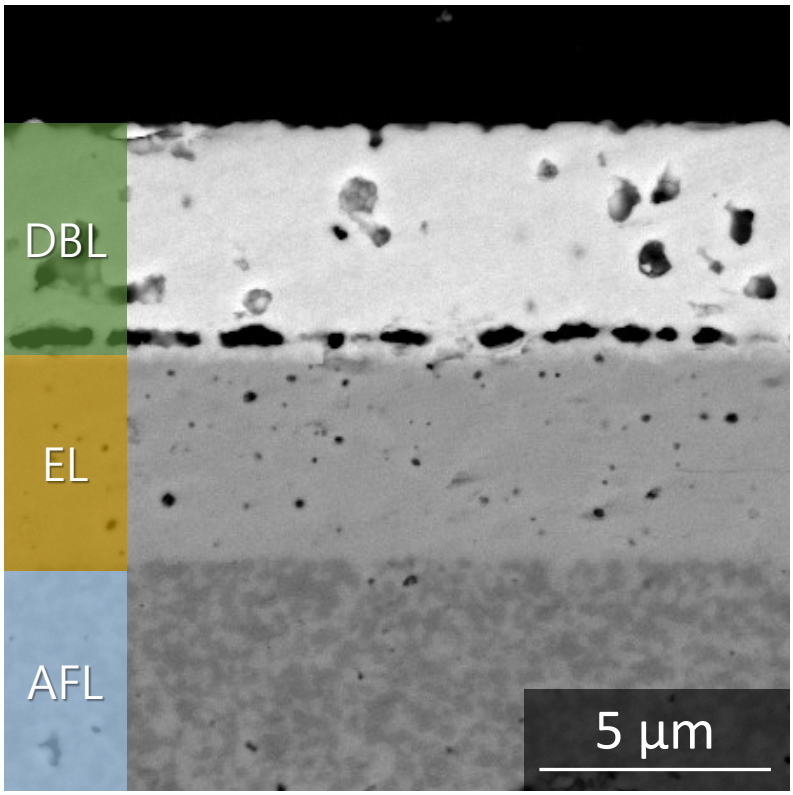

Figure S4. SEM image of GDC diffusion-blocking layer containing 1 wt% Cu as a sintering aid after sintering at 1100 °C. DBL, EL, and AFL refer to diffusion-blocking layer, electrolyte, and anode functional layer, respectively. Although a fairly dense film was formed with the aid of Cu, a significant number of large pores are observed at the interface with the YSZ electrolyte, indicating weak adhesion.

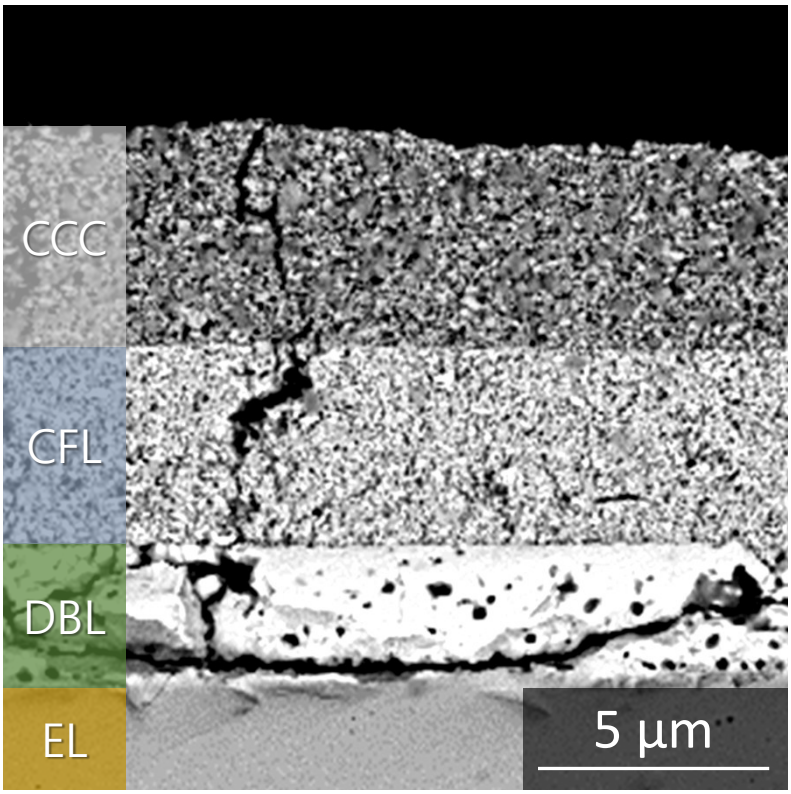

Figure S5. SEM image of the cell incorporating the relatively dense diffusion-blocking layer with interfacial pores. In the GDC diffusion-blocking layer, 1 wt% Cu was added as a sintering aid. This SEM image was taken after cell testing. It clearly shows that the interfacial pores could cause the delamination crack and catastrophic failure. In addition, vertical cracks are also observed, which are considered to have originated from the vertical pores within the diffusion-blocking layer.

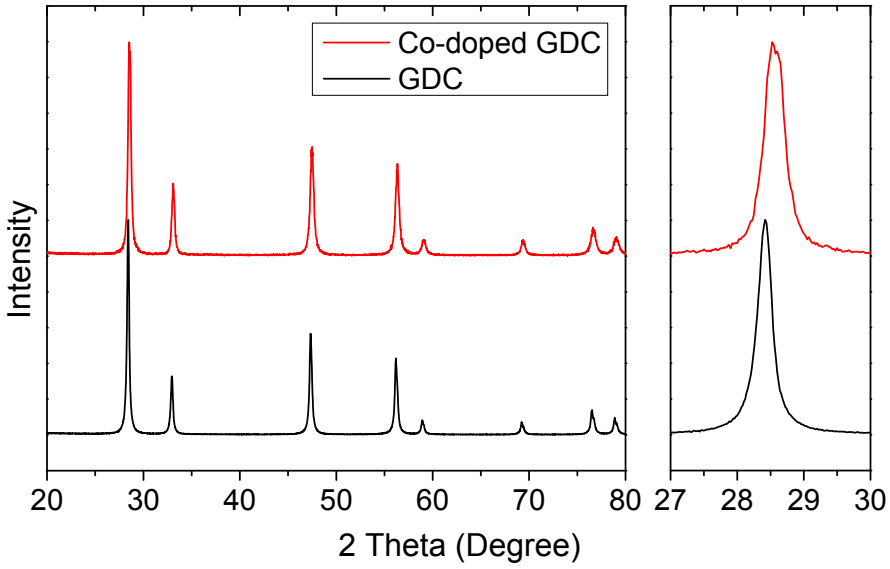

Figure S6. XRD patterns of commercial GDC powder and 1 wt% cobalt-doped GDC powder synthesized by GNP.

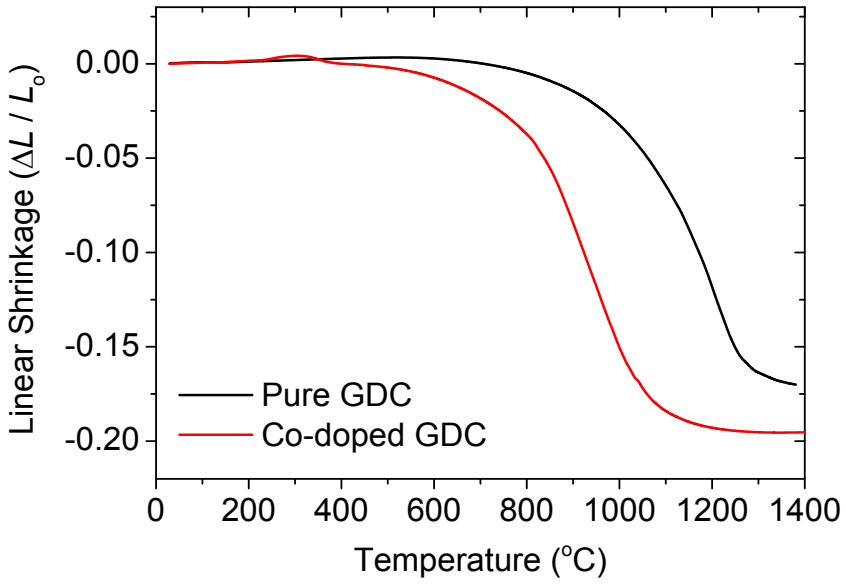

Figure S7. Linear shrinkage curve of the pure GDC and 1 wt% Co-doped GDC measured up to 1400 °C in air.

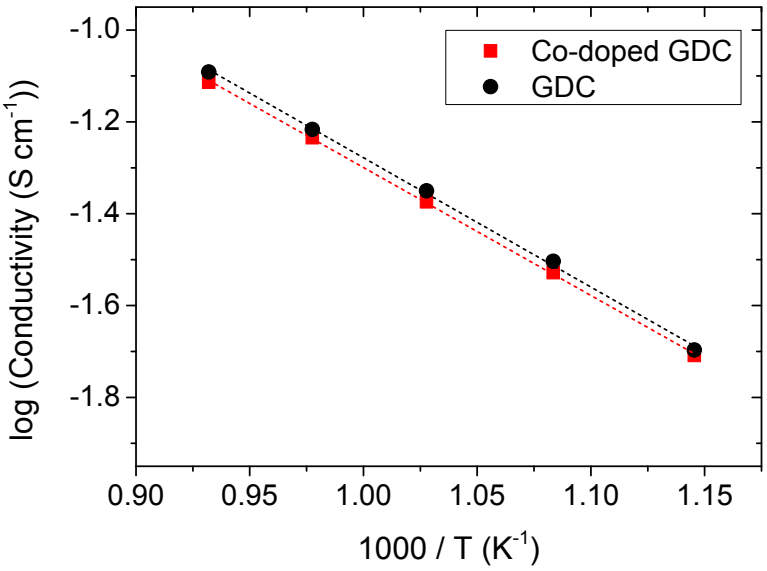

Figure S8. Electrical conductivity of commercial and 1 wt% Co-doped GDC synthesized by GNP. The bar sample with dimensions of 1.5 mm × 5 mm × 15 mm was prepared by uniaxially pressing at 80 MPa and isostatically pressing at 200 MPa, followed by sintering at 1400 and 1200 °C for the commercial and Co-doped GDC, respectively. The conductivity measurement was performed using a four-probe DC technique at 650–850 °C in air.

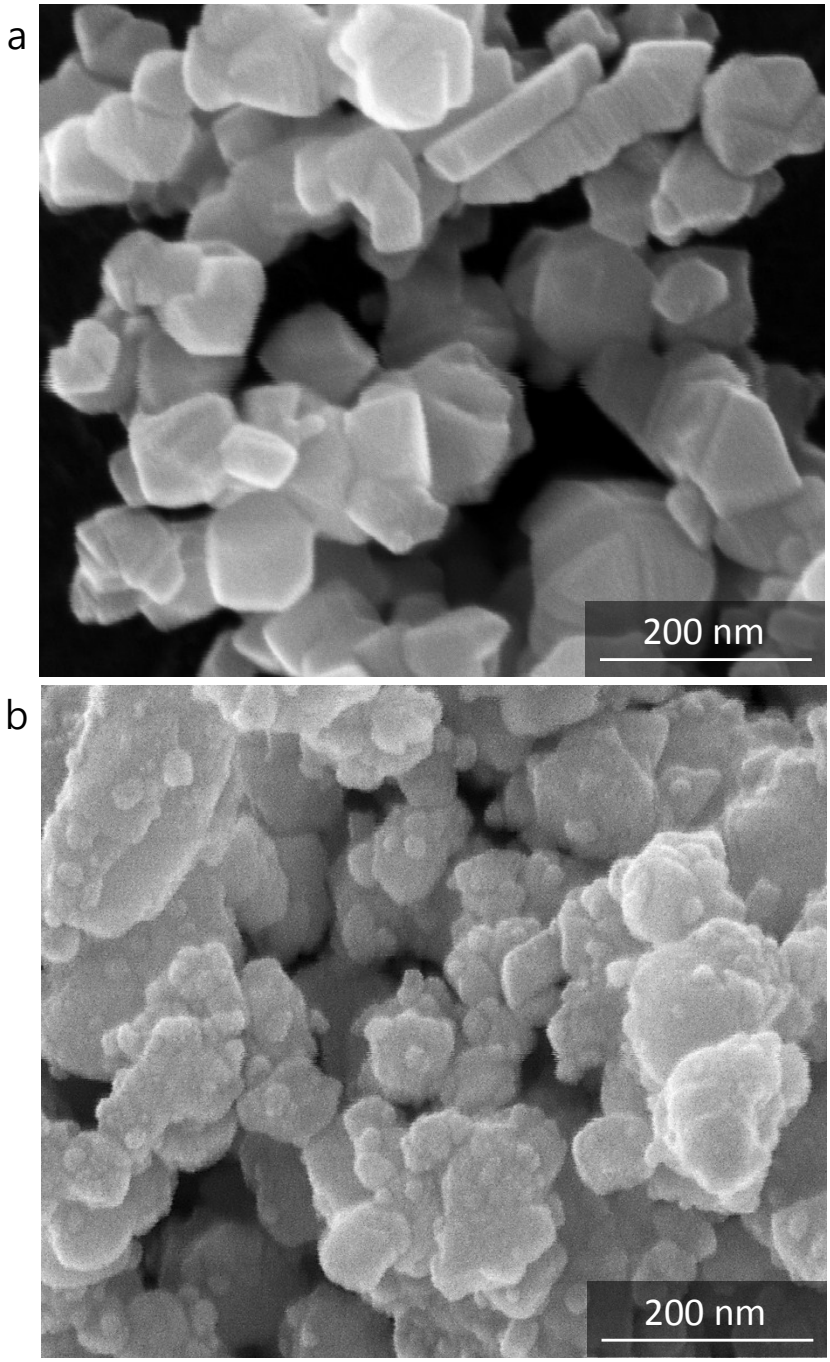

Fig. S9. SEM images of (a) pure coarse particles and (b) nanoparticles conjugated on coarse particles.

a

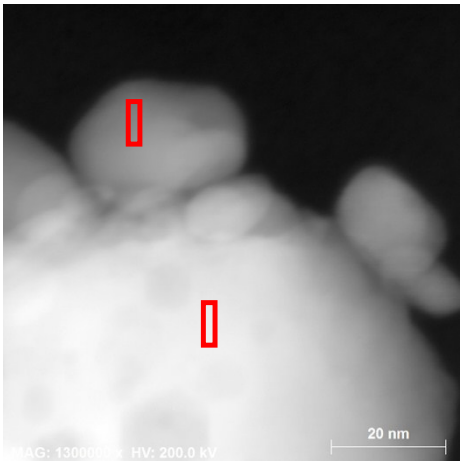

Spot	Ce (At%)	Gd (At%)	O (At%)
1	30.72	3.74	65.54
2	29.98	3.20	66.82

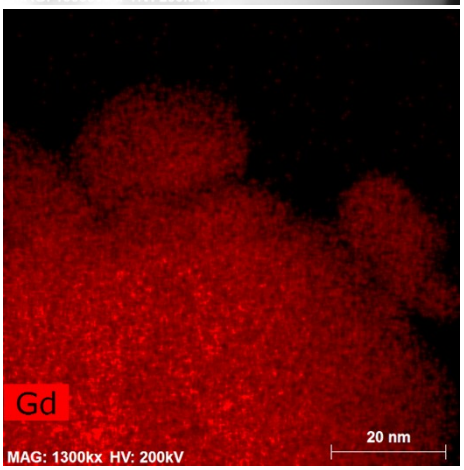

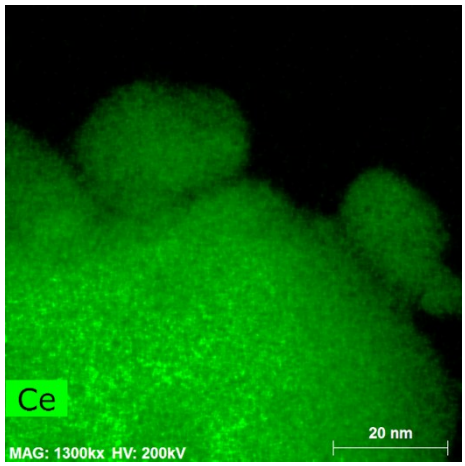

b

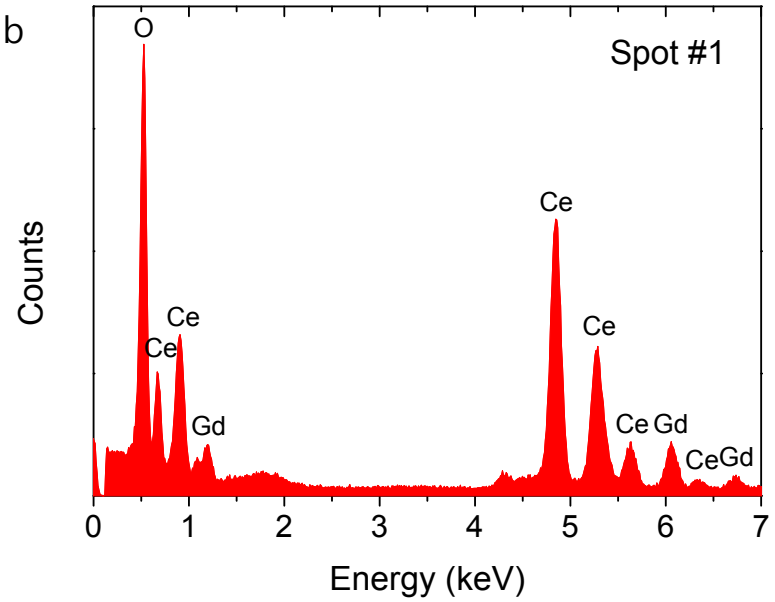

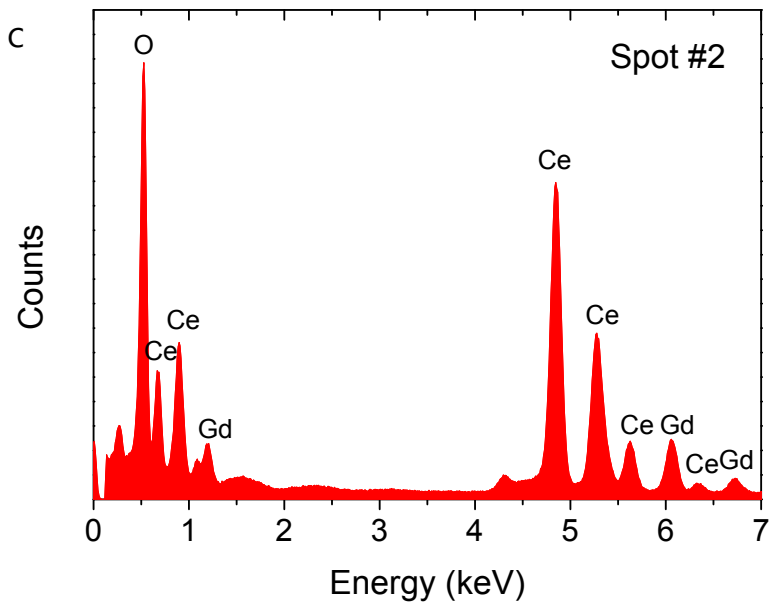

Figure S10. (a) TEM image and elemental analysis of the nanoparticle conjugates synthesized by PD-GNP. (b–c) EDS spectra obtained from spot (b) #1 and (c) #2 in Figure (a).

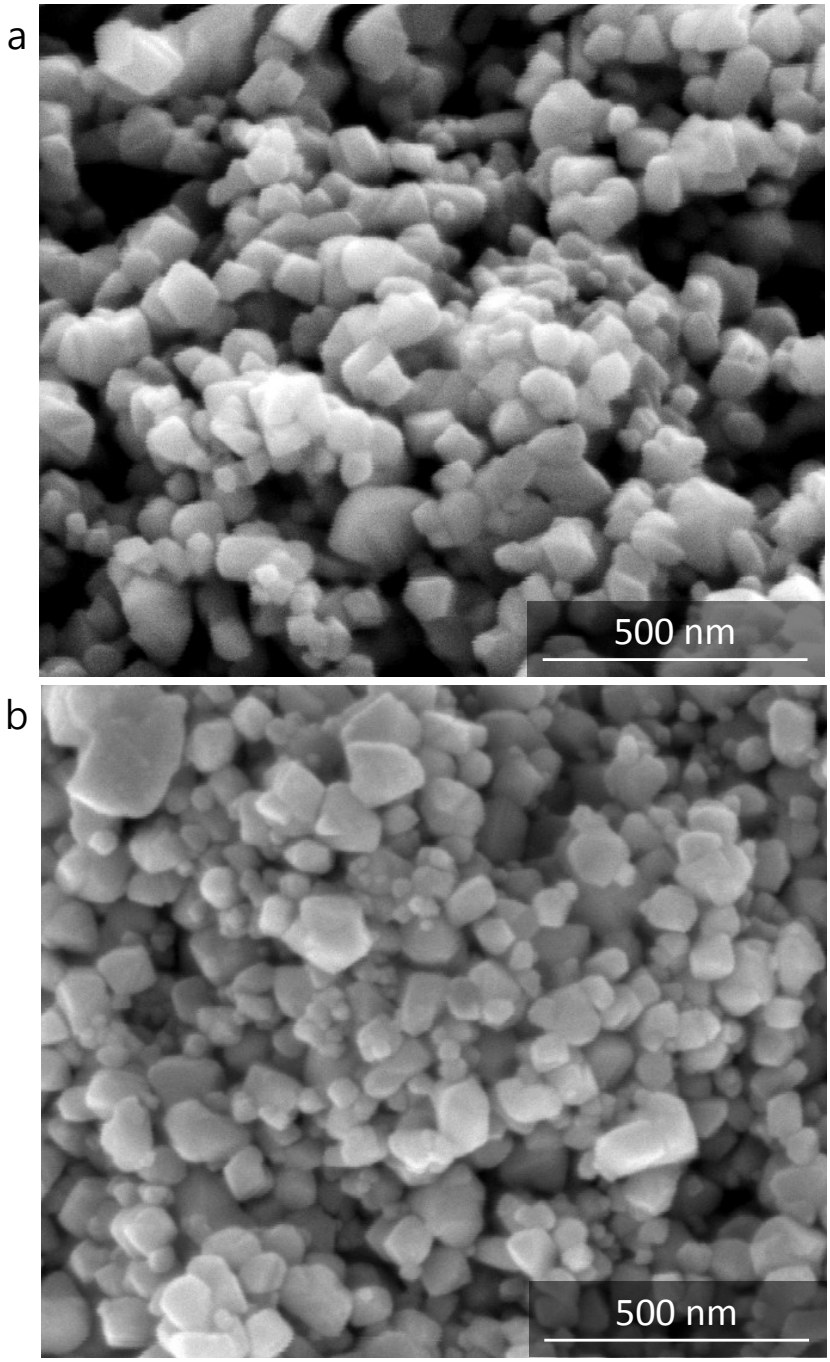

Figure S11. SEM images of the bottom layer composed of (a) 100% coarse particles and (b) 70% coarse particles and 30% nanoparticles. SEM images were taken after the particle rearrangement process at 800 °C for 2 h.

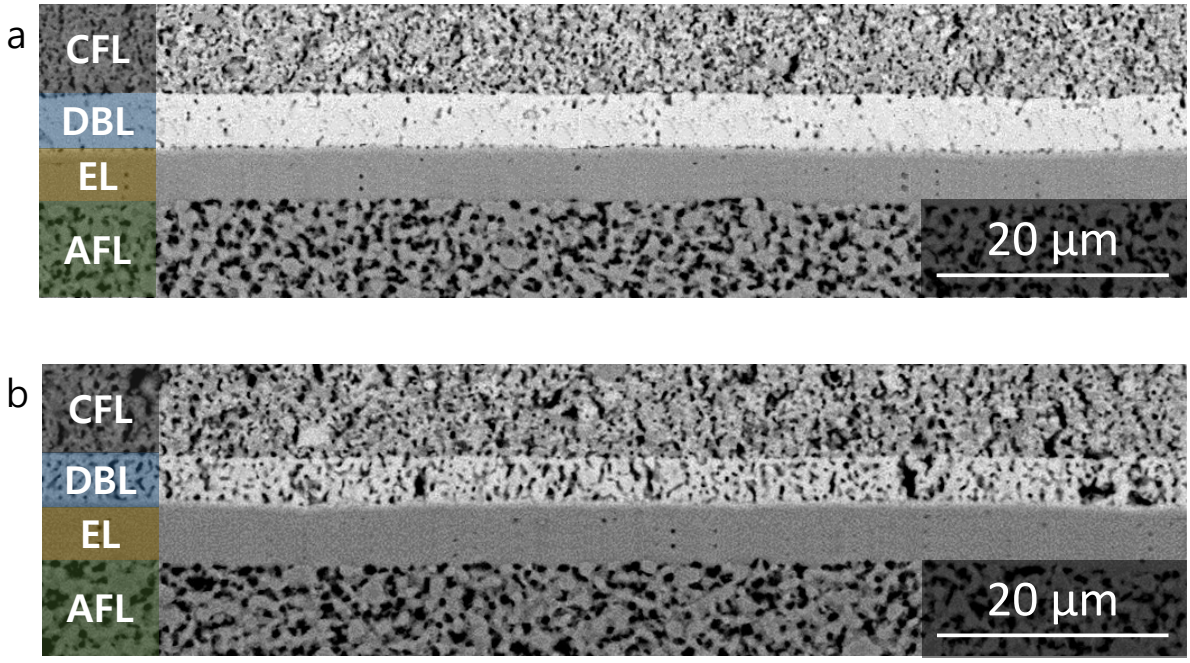

Figure S12. SEM images showing the diffusion-blocking layer fabricated by the (a) bilayer technique and (b) conventional process (CFL: cathode functional layer, DBL: diffusion-blocking layer, EL: electrolyte and AFL: anode functional layer).

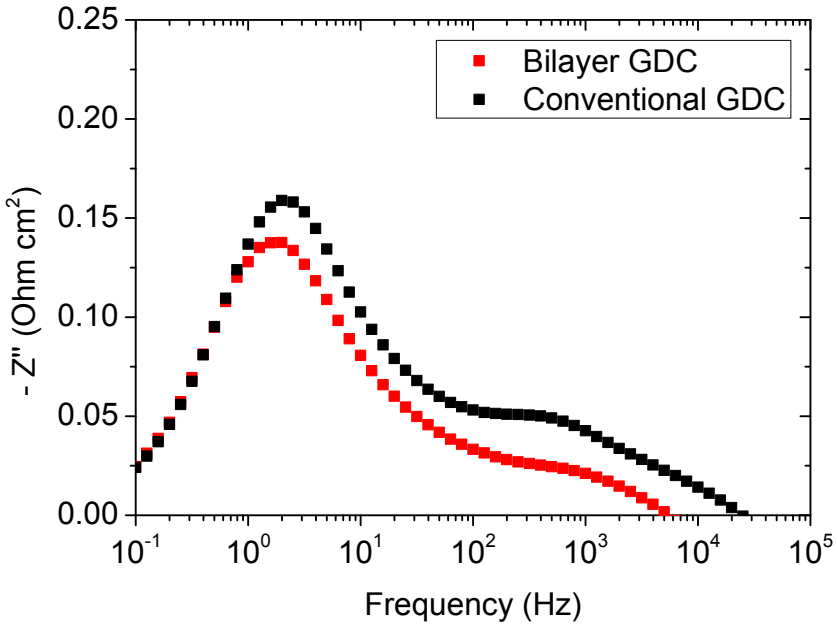

Figure S13. Bode plot of the impedance spectra of the cells with bilayer and conventional GDC diffusion-blocking layer measured at 750 °C.

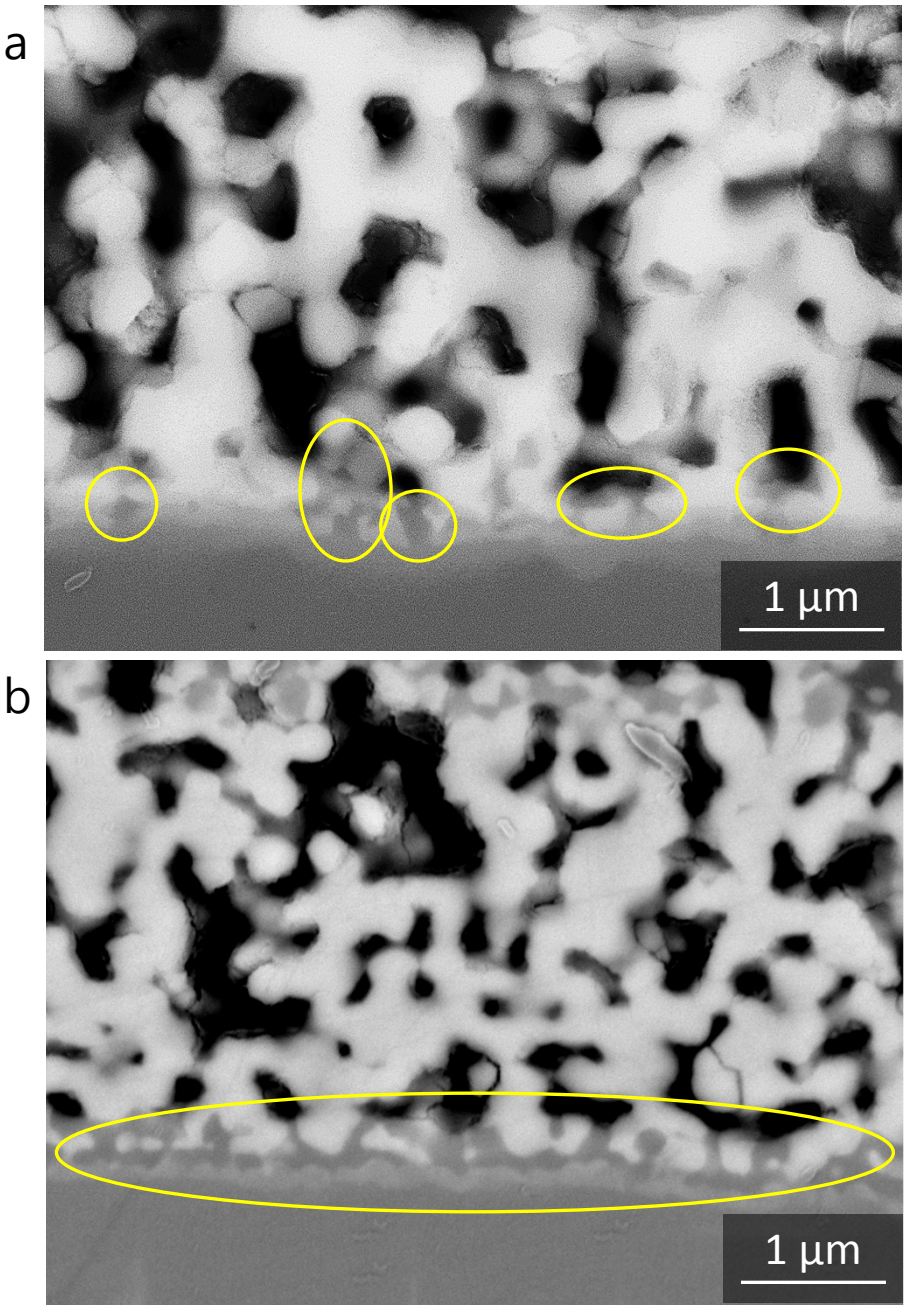

Figure S14. SEM images showing $SrZrO_3$ formed at the interface between the diffusion-blocking layer and electrolyte for the conventional cell after (a) fabrication and (b) long-term operation (dark parts in yellow circles: $SrZrO_3$ phase).